PNAS RESEARCH ARTICLE | MICROBIOLOGY

# Remodeling *Yersinia pseudotuberculosis* to generate a highly immunogenic outer membrane vesicle vaccine against pneumonic plague

Xiuran Wang[a,1], Peng Li[a,1], Amit K. Singh[a], Xiangmin Zhang[b], Ziqiang Guan[c], Roy Curtiss III[d,2], and Wei Sun[a,2]

Edited by Ralph Isberg, Tufts University School of Medicine, Boston, MA; received May 27, 2021; accepted January 21, 2022

**A recombinant enteric *Yersinia pseudotuberculosis* PB1$^+$ strain (Yptb) was designed to synthesize an adjuvant form of lipid A (monophosphoryl lipid A [MPLA]), and tailor an Asd$^+$ plasmid pSMV13 for high synthesis of the *Yersinia pestis* LcrV antigen. The recombinant Yptb mutant harboring the pSMV13 dramatically increased the production of outer membrane vesicles (OMVs) enclosing high amounts of LcrV in comparison to its *Y. pestis* counterpart. Intramuscular (i.m.) immunization with 40 μg of OMVs from YptbS44(pSMV13) (termed OMV$_{YptbS44}$-Bla-V) afforded complete protection to mice against medium (5 ×10$^3$ colony-forming units [CFU], 50 median lethal dose [LD$_{50}$]) and high (400 LD$_{50}$) doses of pulmonary *Y. pestis* infection, as well as against subcutaneous (s.c.) infection with 5 ×10$^5$ CFU (50,000 LD$_{50}$) of *Y. pestis*. In addition, i.m. immunization with 40 μg of detoxified OMVs from YptbS45(pSMV13) (termed OMV$_{YptbS45}$-Bla-V) afforded 90% protection against pulmonary challenge with 50 LD$_{50}$ of *Y. pestis* and complete protection against s.c. challenge with 50,000 LD$_{50}$ of *Y. pestis*. The protective efficacy was superior to that of vaccination with the F1V subunit vaccine or OMVs from a previous recombinant *Y. pestis* strain (termed OMV$_{Yp}$-Bla-V). Further, vaccination with OMV$_{YptbS44}$-Bla-V induced robust humoral and cellular immune responses that were correlated with rapid bacterial clearance, unremarkable tissue damage, and low inflammatory cytokine production in the lungs during pulmonary *Y. pestis* challenge. Our results imply that the recombinant Yptb OMV delivering the *Y. pestis* protective antigen(s) merits further development as a next-generation plague vaccine candidate.**

*Y. pseudotuberculosis* | outer membrane vesicles | monophosphoryl lipid A | plague vaccine | protective immunity

## Significance

*Yersinia pestis*, the etiologic agent of plague, has been responsible for high mortality in several epidemics throughout human history. This plague bacillus has been used as a biological weapon during human history and is currently one of the deadliest biological threats. Currently, no licensed plague vaccines are available in the Western world. Since an array of immunogens are enclosed in outer membrane vesicles (OMVs), immune responses elicited by OMVs against a diverse range of antigens may reduce the likelihood of antigen circumvention. Therefore, self-adjuvanting OMVs from a remodeled *Yersinia pseudotuberculosis* strain as a type of plague vaccine could diversify prophylactic choices and solve current vaccine limitations.

Plague caused by *Yersinia pestis* is responsible for millions of deaths in human history (1). Bubonic plague and pneumonic plague are two primary forms developed in individuals, depending on the route of infection (1). Currently, there are several thousand global cases annually (2), so the plague is widely assumed to be a public health concern of the past. However, as an enzootic vector-borne disease, plague is maintained in natural reservoirs in large rodent populations (3). Fortunately, the fleas that are associated with these rodent reservoir species have little affinity for humans. However, the chance introduction of insect vectors with differing host affinities could adversely alter the potential transmission of *Y. pestis* to humans. In addition, the potential for new outbreaks increases as human territories expand in endemic regions of the world (4–6). Moreover, there are increasing concerns about the occurrence of multiple antibiotic-resistant *Y. pestis* (7) due to the intrinsic genetic plasticity of this bacterium (8). No licensed plague vaccines are currently recommended by the World Health Organization (9). Thus, developing a safe and effective vaccine against pneumonic plague remains of high interest.

In our previous study, it was shown that YPS9, a *Y. pestis* mutant, increased the biogenesis of bacterial OMVs through synthesizing the monophosphoryl lipid A (MPLA), an adjuvant form of lipid A (10). The YPS9 strain harboring an Asd$^+$ plasmid pSMV13 (termed Bla-V) (*SI Appendix*, Table S1), which contains a N-terminal β-lactamase signal sequence (*bla* SS) fused to *Y. pestis lcrV*, could effectively secret LcrV into the periplasm by the type II secretion system (T2SS) and substantially increase the amounts of the LcrV antigen in OMVs (10). Intramuscular (i.m.) immunization with 400 μg of *Y. pestis* OMVs comprising the MPLA and major antigens (LcrV and F1) afforded significant protection of mice against bubonic and pneumonic plague (10). However, our first version of the *Y. pestis*-OMV system suffered several drawbacks: 1) The yield rate of OMVs from YPS9(pSMV13) (termed OMV$_{Yp}$-Bla-V) was relatively low, resulting in the entire process of OMV purification being labor intensive; 2) a low

Author contributions: X.W., P.L., and W.S. designed research; X.W., P.L., A.K.S., X.Z., and Z.G. performed research; X.W., P.L., X.Z., Z.G., R.C., and W.S. analyzed data; X.Z. and W.S. contributed new reagents/analytic tools; and Z.G., R.C., and W.S. wrote the paper.

Conflict of interest statement: R.C. is a cofounder and part owner of Curtiss Healthcare, Inc., which is involved in developing vaccines against infectious diseases of farm animals.

This article is a PNAS Direct Submission.



[1]X.W. and P.L. contributed equally to this work.

[2]To whom correspondence may be addressed. Email: rcurtiss@ufl.edu or sunw@amc.edu.

This article contains supporting information online at http://www.pnas.org/lookup/suppl/doi:10.1073/pnas.2109667119/-/DCSupplemental.

Published March 11, 2022.

ratio of the LcrV antigen was enclosed in OMVs (less than 10 μg of LcrV in 400 μg of OMVs); 3) *Y. pestis* with extensive insertion sequences and loss of hundreds of genes was genetically more unstable than its progenitor *Yersinia pseudotuberculosis* (Yptb) (11), which rendered it problematic to delete *Y. pestis tolR*, *vacJ*, or *yrbE*, which are associated with bacterial membrane curvature for increasing OMV production (laboratory observation); and 4) administration of 400 μg of OMVs for immunization challenged vaccine applicability in humans because the licensed *Neisseria meningitidis* vaccine, Bexsero, includes 25 μg of OMVs from the *N. meningitidis* strain NZ98/254 and 50 μg each of Neisserial Heparin Binding Antigen, Neisseria adhesin A, and Factor H binding protein (12). All of the above issues render the recombinant *Y. pestis* system inferior for OMV preparation and application as a plague vaccine.

Yptb is thought to be the direct evolutionary ancestor of *Y. pestis* (11). The two species share >95% genetic identity and a common virulence plasmid (pCD1/pYV) with a conserved colinear backbone (11). As a food-borne pathogen, Yptb naturally lacks two additional plasmids (pPCP1 and pMT1) carried by *Y. pestis* that encode harmful virulence factors (Pla and Ymt) (13, 14). Additionally, our observations indicated that Yptb grows much faster than *Y. pestis* at 28 °C in heart infusion broth (HIB) medium and is easier to genetically manipulate than *Y. pestis* (laboratory observations), which drove us to remodel Yptb for OMV preparation. Our studies showed that a recombinant YptbS44 strain harboring pSMV13 [YptbS44(pSMV13)] produced substantially higher amounts of OMVs enclosing large amounts of the LcrV antigen than the YPS9(pSMV13) strain. In comparison to administration of OMVs from YPS9(pSMV13) (termed $OMV_{Yp}$-Bla-V) and OMVs from YptbS44(pYA3493) (termed $OMV_{YptbS44}$-NA), i.m. immunization with OMVs from YptbS44(pSMV13) (termed $OMV_{YptbS44}$-Bla-V) induced potent synergistic humoral and cellular responses and afforded excellent protection against pneumonic and bubonic plague. Moreover, i.m. immunization with detoxified OMVs from YptbS45(pSMV13) (termed $OMV_{YptbS45}$-Bla-V) also afforded significant protection against pneumonic and bubonic plague.

## Results

**Construction of a *Y. pseudotuberculosis* Mutant Strain for High Production of Self-Adjuvanting OMVs.** To achieve a genotype similar to that of the *Y. pestis* mutant YPS9 (*SI Appendix*, Table S1) (10), we used the Yptb mutant, χ10061 (*SI Appendix*, Table S1), as a parent strain, in which the *caf1* operon from *Y. pestis* is inserted into and in place of the deleted *lacZ* locus of χ10061 to synthesize the F1 antigen (15). Based on χ10061, the virulence plasmid pYV (~70 kb), which is homologous to pCD1, was cured, and the *hmsHFRS* operon was deleted to generate YptbS41 to eliminate potential adverse effects caused by Yops (*Yersinia* outer proteins) and biofilms contained in OMVs (16). Similar to *Escherichia coli*, Yptb synthesizes the $Kdo_2$-lipid $IV_A$ precursor via sequential reactions; subsequently adds the palmitoleoyl (C16:1) by palmitoleoyltransferase encoded by the *lpxP* gene at 26 °C or below, or laurate (C12:0) at 37 °C by lauroyltransferase encoded by the *lpxL* gene that is absent in *Y. pestis* (17, 18); then stepwise adds myristate (C14:0) by myristoyltransferase encoded by the *lpxM* gene to form hexaacylated lipid A, the lipid component of endotoxin (17). Therefore, directly inserting the $P_{lpp}$ *lpxE* (19) into and in place of the deleted *lacI* locus of YptbS41 to generate YptbS42 may mainly produce 1-dephosphorylated hexaacylated lipid A (MPLA), an adjuvant approved by the Food and Drug Administration (20). In addition, we attempted to delete several conserved genes (*tolR*, *vacJ*, *yrbE*, or *nlpI*) encoding a range of proteins involved in maintaining bacterial membrane integrity (21–24) from *Yersinia* to promote bacterial membrane curvature and further increase the production of OMVs. The results showed that only *tolR* deletion dramatically increased the production of OMVs in Yptb (*SI Appendix*, Fig. S1*A*). Thus, the *tolR* mutation was introduced into YptbS42 to generate YptbS43, but this mutation could not be introduced in the YPS9 strain (laboratory observation). Finally, we introduced Δ*asd* into YptbS43 to generate YptbS44, which could tailor an $Asd^+$ plasmid, pSMV13 (*SI Appendix*, Table S1) (10), for oversynthesis of the *Y. pestis* LcrV antigen.

Accordingly, we then analyzed bacterial morphology via transmission electron microscopy (TEM) and found that the membrane curvature of both YPS9 and YptbS44 harboring the $Asd^+$ plasmid was strikingly increased in comparison to that of the respective wild-type (WT) strains (*SI Appendix*, Fig. S1*B*). YptbS44 harboring an empty $Asd^+$ plasmid pYA3493 [termed YptbS44(pYA3493)] seemed to release more budding structures around bacteria than YPS9(pYA3493) (*SI Appendix*, Fig. S1*B*). Based on total protein analysis, both YptbS44(pSMV13) and YptbS44(pYA3493) yielded higher amounts of OMVs (2.7 and 1.7 mg/L) than YPS9(pSMV13) (0.53 mg/L) (Fig. 1*A*). Comparable high amounts of LcrV were found in bacterial cell lysates (BCLs) of YptbS44(pSMV13) and YPS9(pSMV13), but approximately 10-fold higher amounts of LcrV were enclosed in $OMV_{YptbS44}$-Bla-V than in $OMV_{Yp}$-Bla-V (Fig. 1*B*). No LcrV was detected in BCLs or OMVs from the control strain YptbS44(pYA3494). Considerable amounts of the F1 antigen were detected in the BCL and OMV ($OMV_{Yp}$-Bla-V) of YPS9(pSMV13) strain, but F1 was undetectable in the BCLs of YptbS44(pSMV13), YptbS44(pYA3494), and their OMVs (Fig. 1*B*). Further, we analyzed the proteins in $OMV_{YptbS44}$-Bla-V by mass spectrometry (MS). A total of 450 unique proteins (Dataset S1) were identified and the subcellular localization of each protein was determined based on gene ontology (GO) (cellular component) at UniProt (https://www.uniprot.org/). This analysis indicated that of the 236 proteins with defined GO annotations, 3 were found in the extracellular region, 10 in the outer membrane, 20 in the periplasm, 17 in the plasma membrane, and 136 in cytoplasm (*SI Appendix*, Fig. S1*C*). Moreover, LcrV in the OMVs presented the highest intensity (Dataset S1). Collectively, these results confirmed that OMVs produced by genetically modified Yptb contained significant amounts of the targeted antigen and other proteins. In addition, OMVs isolated from Δ*tolR* Yptb (termed OMV-Δ*tolR* Yptb) and $OMV_{YptbS44}$-Bla-V exhibited similar average sizes in diameter that were 85.53 and 71.99 nm, respectively (*SI Appendix*, Fig. S1*D*).

Then, the lipid A species in OMVs (Fig. 1*C*) isolated from Δ*tolR* $PB1^+$ and YptbS44(pSMV13) were analyzed as described in *SI Appendix*, *Materials and Methods*. Consistent with a previous study (25), the major lipid A species in both OMV-Δ*tolR* Yptb and $OMV_{YptbS44}$-Bla-V were penta- and hexaacylated lipid A with two 4-amino-4-deoxy-L-arabinose (L-Ara4N) moieties (*SI Appendix*, Fig. S2 *A*–*C*). However, significant 1-dephosphorylated tetra- and pentaacylated lipid A species were found in only the $OMV_{YptbS44}$-Bla-V (Fig. 1 *D* and *E*), suggesting that the constitutive expression of *lpxE* (lipid A 1-phosphatase) in the YptbS44(pSMV13) strain could partially remove the 1-phosphate group from lipid A. In addition, $OMV_{YptbS44}$-Bla-V contained other lipids, such as diacylglycerol (DAG), fatty acid (FA), phosphatidylglycerol (PG), cardiolipin (CL), phosphatidylethanolamine

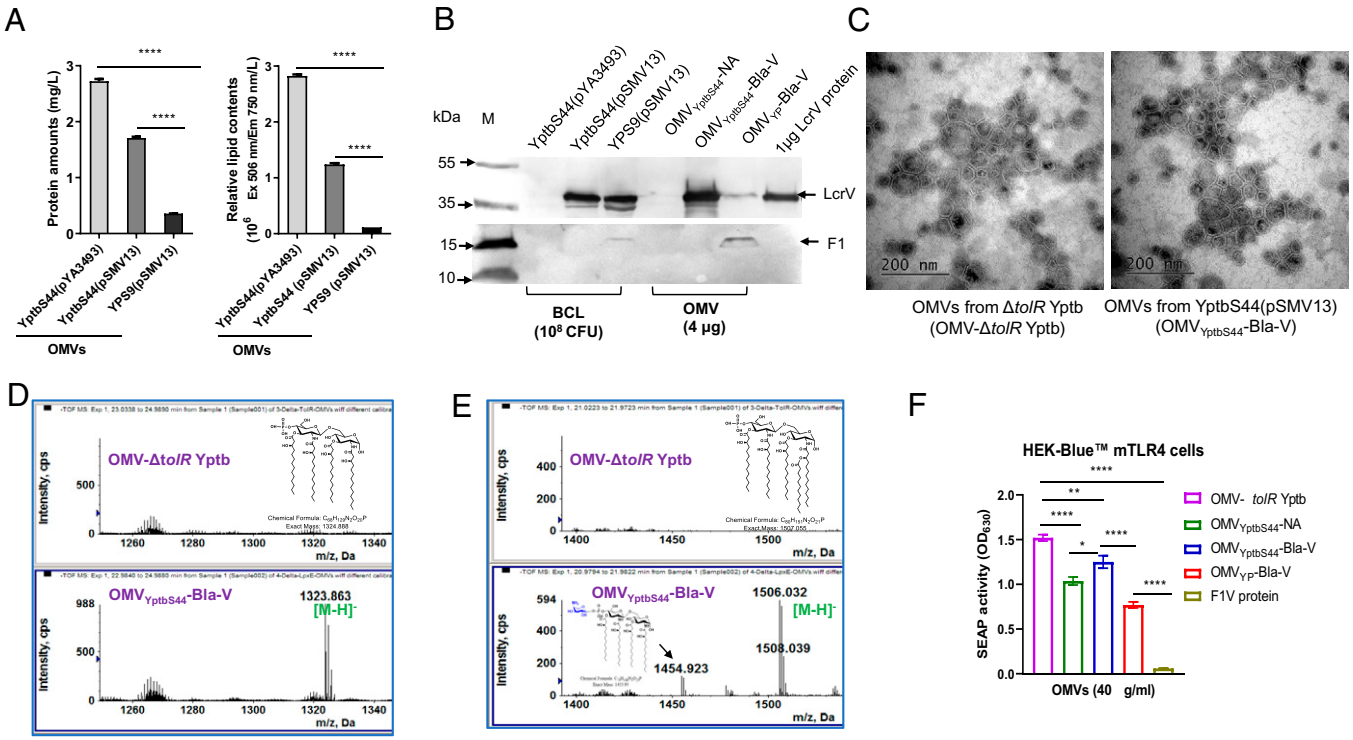


**Fig. 1.** Analysis of OMVs from remodeled *Yersinia*. (*A*) Comparison of OMV production in YptbS44(pSMV13), YptbS44(pYA3493), and YPS9(Bla-V). All the values were normalized according to the total bacterial number (×$10^{11}$ CFU). (*B*) BCLs or OMVs isolated from YptbS44(pSMV13) ($OMV_{YptbS44}$-Bla-V), OMVs from YptbS44(pYA3493) ($OMV_{YptbS44}$-NA), and OMVs from YPS9(pSMV13) ($OMV_{Yp}$-Bla-V) were examined for the presence of LcrV and F1 by immunoblotting. One microgram of purified recombinant LcrV (rLcrV) was used as a loading control. (*C*) TEM images of OMVs purified from Δ*tolR* Yptb and YptbS44(pSMV13). The samples were prepared by conventional staining with 1% aqueous uranyl acetate as described in the *Materials and Methods*. (Scale bars, 500 nm.) The results are representative of three repeated experiments. (*D* and *E*) MS analysis of lipid A species in OMVs from the Δ*tolR* Yptb strain (OMV-Δ*tolR* Yptb) and OMVs from the YptbS44(pSMV13) strain ($OMV_{YptbS44}$-Bla-V). The 1-dephosphorylated tetra- and pentaacylated lipid A species are present in the $OMV_{YptbS44}$-Bla-V but absent in the OMV-Δ*tolR* Yptb. (*F*) Comparison of the SEAP activities in HEK-blue cells with or without murine toll-like receptor 4. HEK-blue mTLR4 (InvivoGen) cells were cocultured with 4 μg/mL of $OMV_{YptbS44}$-Bla-V, $OMV_{YptbS44}$-NA, or $OMV_{Yp}$-Bla-V for 8 h. OMVs from Δ*tolR* Yptb and purified F1V were used as controls. Data are shown as the mean ± SD. The statistical significance of differences among groups was analyzed by two-way multivariate ANOVA with Tukey's post hoc test: *$P < 0.05$; **$P < 0.01$; ***$P < 0.001$; ****$P < 0.0001$.

(PE), lyso-phosphatidylethanolamine (LPE), and phosphatidylcholine (PC) (*SI Appendix*, Fig. S2*D* and Table S3). To further reduce the toxicity of hexaacylated lipid A, we introduced both *lpxL* and *lpxP* mutations on the top of YptbS44 to construct YptbS45 (*SI Appendix*, Table S1). The lipid A species in OMVs isolated from YptbS45(pSMV13) (termed $OMV_{YptbS45}$-Bla-V) predominantly contained monophosphate tetraacylated lipid A (*SI Appendix*, Fig. S2*E*). Further, we compared the secreted embryonic alkaline phosphatase (SEAP) activity of HEK-blue mTLR4 cells cultured with different OMVs. The results showed that the TLR4 stimulatory activity of $OMV_{YptbS44}$-Bla-V or $OMV_{YptbS44}$-NA was significantly less than that of OMV-Δ*tolR* Yptb, whereas substantially higher than that of $OMV_{YP}$-Bla-V or $OMV_{YptbS45}$-Bla-V (Fig. 1*F* and *SI Appendix*, Fig. S2*F*). Moreover, the TLR4 stimulatory activity of $OMV_{YptbS45}$-Bla-V was substantially lower than that of $OMV_{YP}$-Bla-V (*SI Appendix*, Fig. S2*F*). The amount of LcrV contained in $OMV_{YptbS45}$-Bla-V was comparable to that of $OMV_{YptbS44}$-Bla-V (*SI Appendix*, Fig. S2*G*).

**Comparison of Protective Immunity against Pneumonic Plague in Mice Induced by Intramuscular Immunization.** In a previous study, we immunized animals with a very high dose of OMVs (400 μg) from YPS9(pSMV13) (10). To reduce potential toxicity and reactogenicity, we compared the antiplague immunity of different OMVs using lower immunization doses. Groups of mice ($n = 10$, equal males and females) were intramuscularly immunized with 40 μg of $OMV_{YptbS44}$-Bla-V, 40 μg of $OMV_{YptbS44}$-NA, 40 μg of $OMV_{Yp}$-Bla-V, 10 μg of F1V/Alhydrogel (F1V) or phosphate buffered saline (PBS)/Alhydrogel (PBS), and intramuscularly boosted at 21 d after the priming immunization (Fig. 2*A*). Compared to the other immunizations, vaccination with 40 μg of either $OMV_{YptbS44}$-Bla-V or $OMV_{YptbS44}$-NA significantly affected mouse weight gain (Fig. 2*B*), leading to anorexia in 2 d postimmunization, and moderate swelling at the injection site 1 wk after injection (observation data). Whereas weight gain in mice vaccinated with 40 μg of detoxified $OMV_{YptbS45}$-Bla-V or reduced doses of $OMV_{YptbS44}$-Bla-V (20 μg or 10 μg) was comparable to that of F1V (*SI Appendix*, Fig. S3 *A* and *B*) without any observable side effects (observation data). In comparison to PBS, F1V, or $OMV_{YptbS45}$-Bla-V immunization, $OMV_{YptbS44}$-Bla-V immunization induced significantly high levels of IL-6 and IL-1β in sera on days 1 and 3 postimmunization (*SI Appendix*, Fig. S3*C*). Overall, all immunization did not cause any other observable health issues in mice.

On day 42 after the initial vaccination, the mice were challenged with a lethal dose of *Y. pestis* KIM6$^+$(pCD1Ap) by intranasal (i.n.) instillation, mimicking pneumonic plague. The results showed that vaccination with 40 μg of $OMV_{YptbS44}$-Bla-V afforded complete protection against $5 \times 10^3$ colony-forming units (CFU) (50 median lethal dose [$LD_{50}$]) of wild-type *Y. pestis* (Fig. 2*C*), whereas only 20% of F1V-immunized mice and none of the PBS-, $OMV_{YptbS44}$-NA-, or $OMV_{Yp}$-Bla-V–vaccinated mice survived the same challenge (Fig. 2*C*). Moreover, mice immunized with 40 μg of $OMV_{YptbS44}$-Bla-V all survived an i.n. challenge with a high dose ($4 \times 10^4$ CFU, 400 $LD_{50}$) of wild-type *Y. pestis* (Fig. 2*D*).

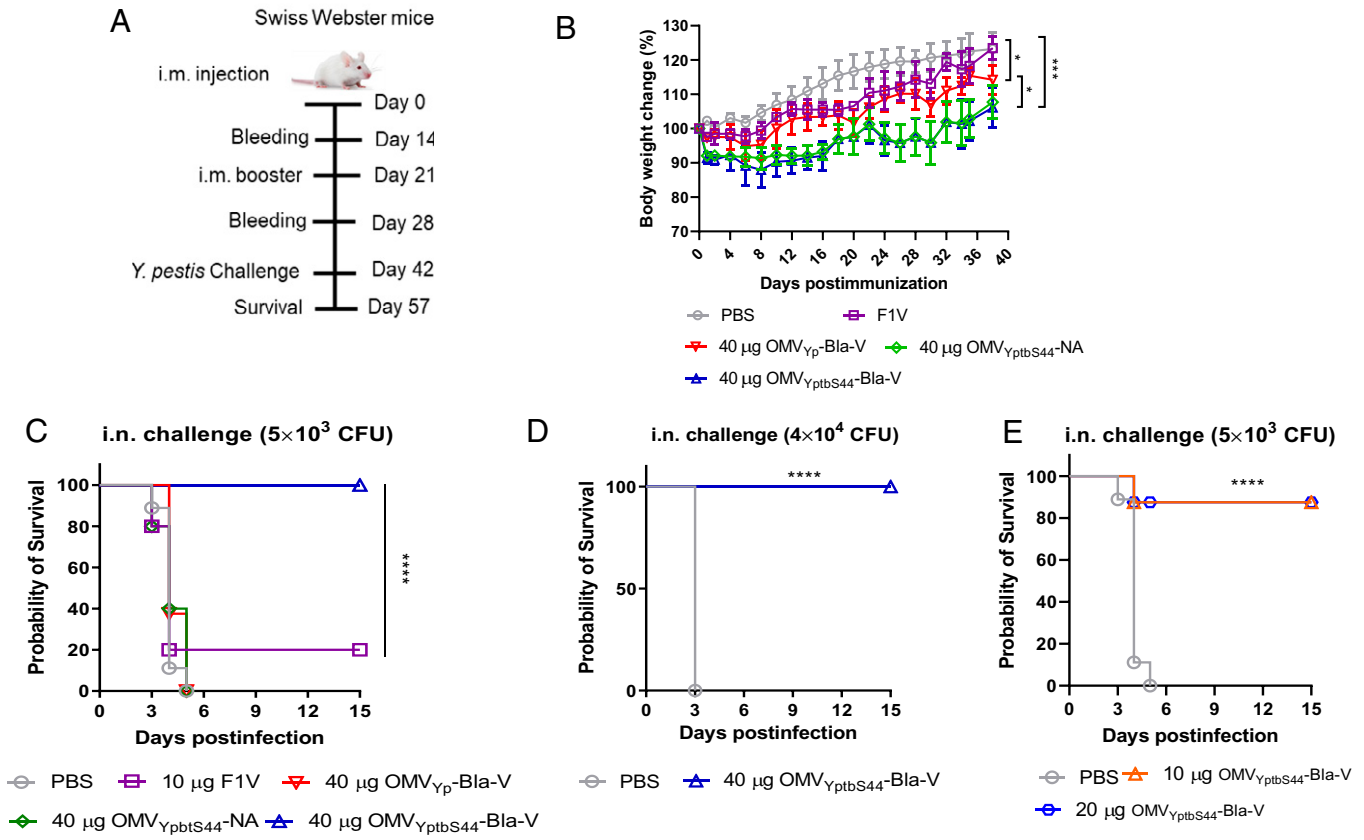


**Fig. 2.** Protective efficacy of i.m. immunization against pneumonic plague. Swiss Webster mice ($n$ = 10, equal numbers of males and females) were immunized intramuscularly with 40 μg of $OMV_{YptbS44}$-Bla-V/100 μL of PBS, 40 μg of $OMV_{YptbS44}$-NA/100 μL of PBS, 40 μg of $OMV_{Yp}$-Bla-V/100 μL of PBS, 10 μg of F1V/Alhydrogel/100 μL of PBS, or Alhydrogel alone/100 μL of PBS (negative control) and then boosted on day 21 after the priming immunization. (*A*) Immunization scheme used for the mouse study. (*B*) Weight change rates of mice after immunization. (*C*) On day 42 after the initial immunization, Swiss Webster mice were intranasally challenged with 5 × $10^3$ CFU of *Y. pestis* $KIM6^+$(pCD1Ap) (50 $LD_{50}$). (*D*) At 42 d after the initial immunization, mice immunized with 40 μg of $OMV_{Yptb}$-Bla-V were intranasally challenged with 400 $LD_{50}$ of *Y. pestis* $KIM6^+$(pCD1Ap). (*E*) On day 42 after the initial immunization, mice vaccinated with 10 or 20 μg of $OMV_{Yptb}$-Bla-V were intranasally challenged with 50 $LD_{50}$ of *Y. pestis* $KIM6^+$(pCD1Ap). The $LD_{50}$ value of *Y. pestis* $KIM6^+$(pCD1Ap) administered by i.n. challenge to mice was ~100 CFU (56). The experiments were performed twice, and the data were combined for analysis. Statistical significance was analyzed by the log-rank (Mantel–Cox) test: ns, no significance; *$P$ < 0.05; **$P$ < 0.01; ****$P$ < 0.0001.

Vaccinations with either reduced doses of $OMV_{YptbS44}$-Bla-V or with 40 μg of detoxified $OMV_{YptbS45}$-Bla-V afforded 90% protection against pulmonary challenge with 50 $LD_{50}$ of wild-type *Y. pestis* (Fig. 2*E* and *SI Appendix*, Fig. S3*D*). In addition, mice vaccinated with either $OMV_{YptbS44}$-Bla-V (10, 20, or 40 μg) or 40 μg of $OMV_{YptbS45}$-Bla-V all survived the subcutaneous (s.c.) challenge with 5 × $10^5$ CFU (5 × $10^4$ $LD_{50}$) of wild-type *Y. pestis*. While 80% of F1V-immunized mice survived, no PBS-, $OMV_{YptbS44}$-NA–, or $OMV_{Yp}$-Bla-V–immunized mice survived the same s.c. challenges (*SI Appendix*, Fig. S3 *E* and *F*).

**Comparison of Protective Immunity against Pneumonic Plague in Mice Induced by Intranasal Immunization.** Respiratory vaccine delivery is considered the most effective route to activate a local immune response in addition to a systemic immune response (26). Therefore, we also tested the protective efficacy of OMVs administered by i.n. immunization. Groups of mice ($n$ = 10) were intranasally immunized with 16 μg of $OMV_{YptbS44}$-Bla-V, 16 μg of $OMV_{YptbS44}$-NA, 16 μg of $OMV_{Yp}$-Bla-V, 5 μg of F1V or PBS, and boosted at 21 d after the priming immunization (Fig. 3*A*). The i.n. immunization with 16 μg of $OMV_{YptbS44}$-Bla-V caused obvious weight loss in the mice after immunization (Fig. 3*B*). Two mice succumbed after an i.n. booster immunization, but the remaining mice did not show observable health issues. An i.n. immunization with a reduced dose of $OMV_{YptbS44}$-Bla-V (8 μg or 4 μg) had effects on mouse weight gain similar to those observed for immunization with 16 μg of $OMV_{Yp}$-Bla-V or 5 μg of F1V (*SI Appendix*, Fig. S4 *A* and *B*). Then, the pulmonary challenge showed that the surviving mice immunized with 16 μg of $OMV_{YptbS44}$-Bla-V all survived, and 40% of the mice immunized with 16 μg of $OMV_{Yp}$-Bla-V survived the i.n. challenge with 50 $LD_{50}$ of wild-type *Y. pestis*, while the F1V-immunized mice barely survived the same challenge (Fig. 3*C*). Immunization with 8 μg of $OMV_{YptbS44}$-Bla-V offered only 50% protection against pulmonary challenge, while immunization with 4 μg of $OMV_{YptbS44}$-Bla-V failed to provide any protection (Fig. 3*D*). None of the PBS- or $OMV_{YptbS44}$-NA–immunized mice survived the same i.n. challenge (Fig. 3 *C* and *D*). Additionally, bubonic challenge showed that i.n. vaccination with 8 or 16 μg of $OMV_{YptbS44}$-Bla-V afforded 50 to 60% protection against 5 × $10^4$ $LD_{50}$ of wild-type *Y. pestis* and 20% of F1V-immunized mice survived the same challenge, while vaccination with 16 μg of $OMV_{Yp}$-Bla-V or 4 μg of $OMV_{YptbS44}$-Bla-V failed to offer any protection. None of the PBS- or $OMV_{YptbS44}$-NA–immunized mice survived the s.c. challenge (*SI Appendix*, Fig. S4 *C* and *D*). Based on the above results, i.m. immunization with $OMV_{YptbS44}$-Bla-V offered better protection against pneumonic and bubonic plague than i.n. immunization. So, we only evaluated immune responses in mice treated by i.m. immunization in subsequent studies.

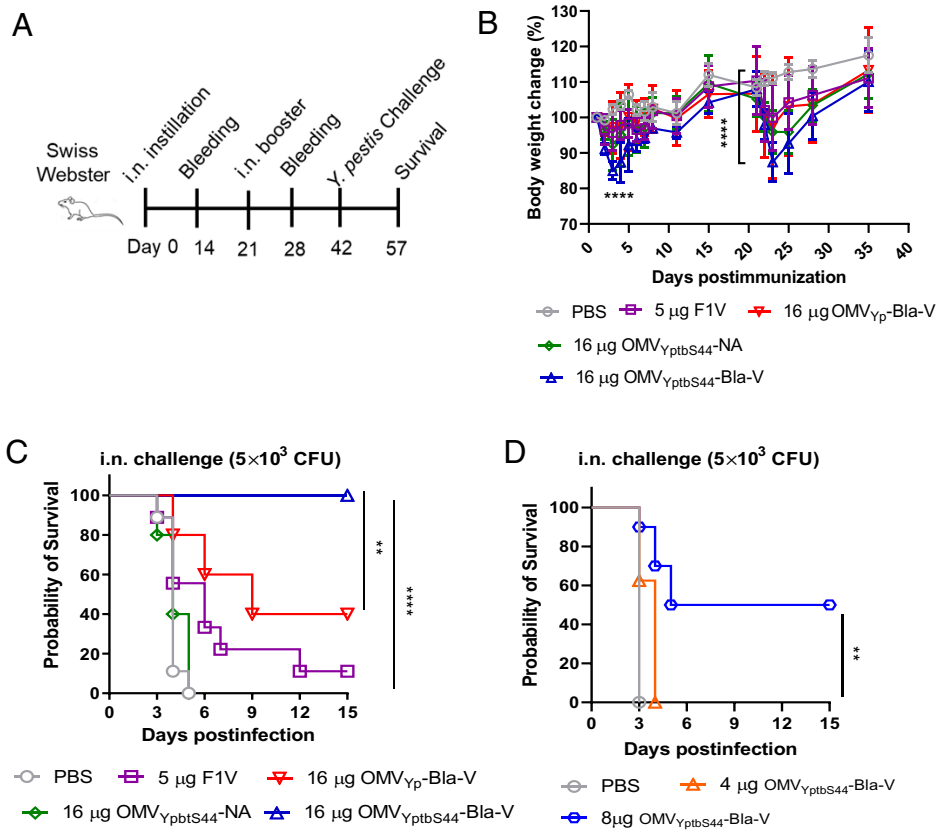


**Fig. 3.** Protective efficacy of i.n. immunization against pneumonic plague. Swiss Webster mice ($n$ = 10, equal numbers of males and females) were immunized intranasally with 16 μg of OMV$_{YptbS44}$-Bla-V/30 μL of PBS, 16 μg of OMV$_{YptbS44}$-NA/30 μL of PBS, 16 μg of OMV$_{Yp}$-Bla-V/30 μL of PBS, 5 μg of F1V/Alhydrogel/30 μL of PBS, or Alhydrogel alone/30 μL of PBS (negative control) and boosted on day 21 after the priming immunization. (*A*) Immunization scheme used for the mouse study. (*B*) Weight change rates of mice after i.n. immunization. (*C*) On day 42 after the initial immunization, mice were intranasally challenged with 50 $LD_{50}$ of *Y. pestis* KIM6$^+$(pCD1Ap). (*D*) On day 42 after the initial immunization, mice vaccinated with 4 or 8 μg of OMV$_{Yptb}$-Bla-V were intranasally challenged with 50 $LD_{50}$ of *Y. pestis* KIM6$^+$(pCD1Ap). The experiments were performed twice, and the data were combined for analysis. Statistical significance was analyzed by the log-rank (Mantel–Cox) test: ns, no significance; *$P$ < 0.05; **$P$ < 0.01; ****$P$ < 0.0001.

**Strong Antibody Responses Induced by i.m. OMV$_{YptbS44}$-Bla-V Vaccination.** Antibody analysis demonstrated that levels of serum anti-LcrV IgG were comparable between mice immunized with 40 μg of OMV$_{YptbS44}$-Bla-V or 10 μg of F1V. The levels were significantly higher than those in mice immunized with 40 μg of OMV$_{Yp}$-Bla-V or 40 μg of OMV$_{YptbS44}$-NA at week 2 postimmunization (Fig. 4*A*). Titers of anti-LcrV IgG were boosted in all vaccinated groups by week 4 postimmunization; however, titers of anti-LcrV IgG in the 40 μg of OMV$_{YptbS44}$-Bla-V–immunized mice were substantially higher than in the other immunized mice (Fig. 4*A*). In general, the subtypes of antigen-specific IgG antibodies can distinguish Th1 and Th2 responses in immunized mice. IgG1 is associated with a Th2-like response, while IgG2a is associated with a Th1 response (27). Experimental results indicated that the anti-LcrV IgG2a/IgG1 ratios in all OMV-immunized groups were equal to or greater than one at both week 2 and week 4 postimmunization and were significantly greater than the ratios (0.49 and 0.65) in the F1V-immunized group (Fig. 4*B*). The results suggested that i.m. OMV immunization generated Th1-biased or balanced Th1/Th2 responses, while F1V immunization stimulated a Th2-biased response. Furthermore, measurement of IgM titers showed that significantly higher titers of anti-LcrV IgM were induced in the 40 μg of OMV$_{YptbS44}$-Bla-V–immunized mice at week 2 postvaccination and maintained after receiving the booster at week 4 postimmunization (Fig. 4*C*). Titers of anti-LcrV IgM in other immunized mice were substantially lower (Fig. 4*C*). Nevertheless, the anti-F1 IgG titers in F1V- or OMV$_{Yp}$-Bla-V–immunized mice were comparable but substantially higher than those in OMV$_{YptbS44}$-NA- or OMV$_{YptbS44}$-Bla-V–immunized mice at week 2 postimmunization (Fig. 4*D*). No anti-F1 IgG titers were observed to be boosted in the OMV$_{YptbS44}$-NA– or OMV$_{YptbS44}$-Bla-V–immunized mice due to very low amounts of F1 enclosed in these OMVs (Fig. 1*B*), and only titers of anti-F1 IgG in either F1V- or OMV$_{Yp}$-Bla-V–vaccinated mice were boosted at week 4 postimmunization (Fig. 4*D*). Titers of anti-*Y. pestis* whole cell lysate (YpL) IgG in all OMV-vaccinated mice were comparable at week 2 postimmunization, boosted at week 4 postimmunization, and significantly higher than those in F1V-immunized mice (Fig. 4*E*). Additionally, i.n. immunization with 16 μg of OMV$_{YptbS44}$-Bla-V–induced patterns of LcrV and F1 antibody titers in mice similar to those induced by i.m. immunization with 40 μg of OMV$_{YptbS44}$-Bla-V (*SI Appendix*, Fig. S5).

**Potent CD4 T Cell Responses Induced by i.m. OMV$_{YptbS44}$-Bla-V Vaccination.** Given that T cells mainly contribute to protection against pulmonary *Y. pestis* infection (28), we determined whether lung T cell responses could be enhanced in immunized mice upon *Y. pestis* infection. CD44 is one of the most used activation markers for T cells. Upon antigen encounter, memory T cells rapidly up-regulate CD44 (29). Before i.n. *Y. pestis* challenge, numbers of CD4$^+$ CD44$^+$ cells in the lungs of all vaccinated mice were higher than those in the lungs of PBS-vaccinated mice, while the number of CD8$^+$ CD44$^+$ cells was not different among the groups (*SI Appendix*, Fig. S6 *A* and *B*).

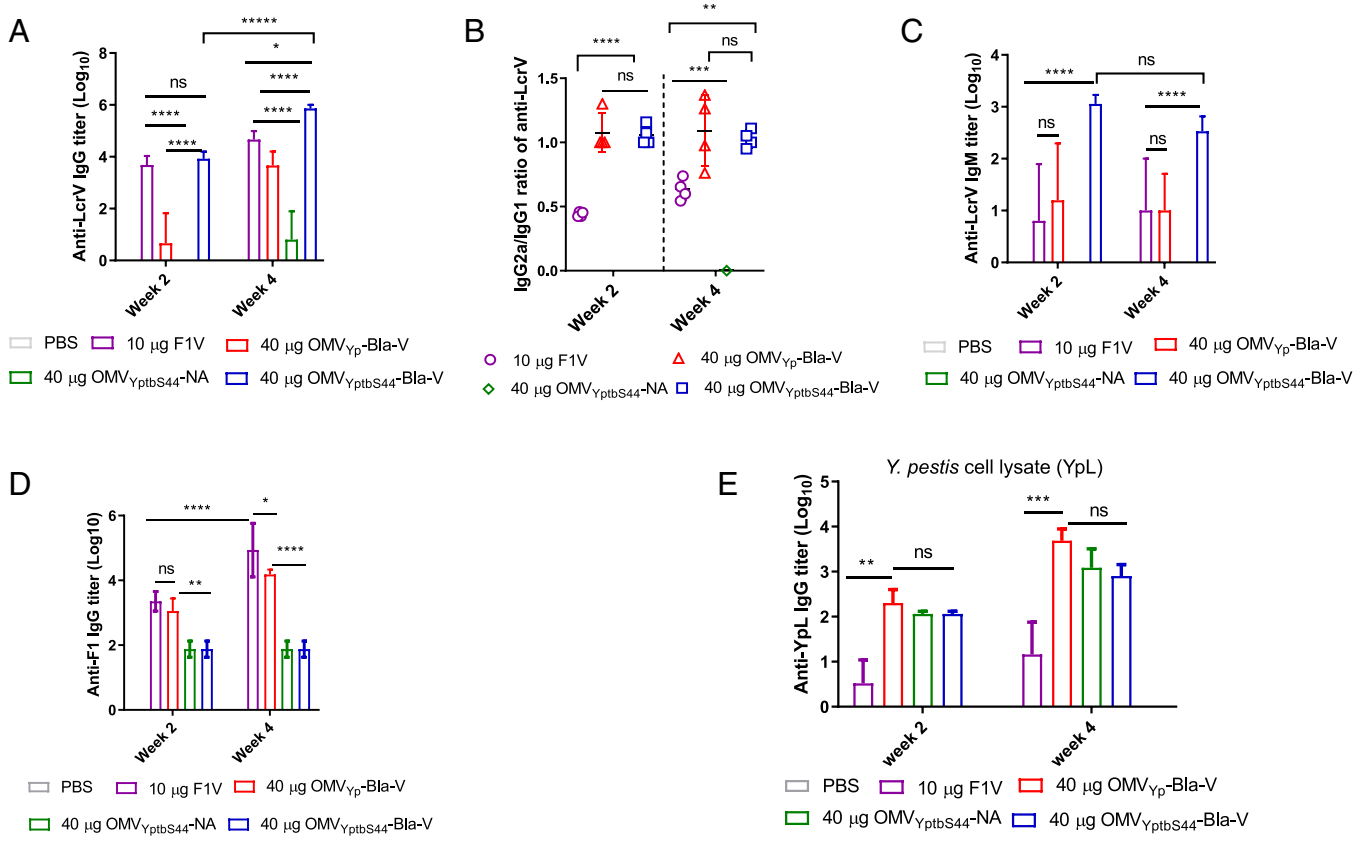


**Fig. 4.** Antibody responses to LcrV and F1 in mice induced by i.m. immunization. Swiss Webster mice ($n$ = 10, equal numbers of males and females) were immunized intramuscularly with 40 μg of $OMV_{YptbS44}$-Bla-V/100 μL of PBS, 40 μg of $OMV_{YptbS44}$-NA/100 μL of PBS, 40 μg of $OMV_{Yp}$-Bla-V/100 μL of PBS, 10 μg of F1V/Alhydrogel/100 μL of PBS, or Alhydrogel alone/100 μL of PBS (negative control) and then boosted on day 21 after the priming immunization. Blood was collected on weeks 2 and 4 for antibody analysis. Data represent 10 mice per group. (*A*) Anti-LcrV total IgG titers on weeks 2 and 4 in different immunized mice. (*B*) Ratios of IgG2a/IgG1 for antibodies specific for the LcrV antigen on weeks 2 and 4. (*C*) Anti-LcrV IgM titers on weeks 2 and 4 in different immunized mice. (*D*) Anti-F1 total IgG titers on weeks 2 and 4 in different immunized mice. (*E*) Anti-YpL total IgG titers on weeks 2 and 4 in different immunized mice. Data are shown as the mean ± SD. The statistical significance of differences among groups was analyzed by two-way multivariate ANOVA with Tukey's post hoc test: ns, no significance; *$P$ < 0.05; **$P$ < 0.01; ***$P$ < 0.001; ****$P$ < 0.0001.

Three days after i.n. challenge with 5 × $10^6$ CFU of $Pgm^-$ *Y. pestis*, the population of $CD44^+$ T cells in the lungs of different immunized mice was analyzed using flow cytometry (Fig. 5*A*). Quantitative analysis showed that the number of $CD4^+$ $CD44^+$ cells in the $OMV_{YptbS44}$-Bla-V–immunized mice was increased by 4-fold, and the number of $CD8^+$ $CD44^+$ cells was increased by 1.2-fold compared with that in the other immunized mice (Fig. 5*B*). Cytokines, such as IFN-γ, IL-17A, and TNF-α, are required for T cell–mediated protection against pneumonic plague (30, 31). Therefore, we determined the capacity of T cells to produce IFN-γ, IL-17A, or TNF-α before or after in vivo activation using flow cytometry (Fig. 5*C*). Before i.n. *Y. pestis* challenge, the numbers of $CD4^+$ and $CD8^+$ cells producing IFN-γ, IL-17A, or TNF-α were very low and not significantly different among the groups (*SI Appendix*, Fig. S6 *C–F*). However, 3 d after pulmonary *Y. pestis* infection, we observed dramatic increases in the numbers of IFN-γ–, IL-17A– and TNF-α–producing $CD4^+$ T cells in $OMV_{YptbS44}$-Bla-V–immunized mice compared to PBS-, F1V- or $OMV_{Yp}$-Bla-V–immunized mice (Fig. 5*D*). Numbers of IL-17A–producing CD4 T cells in F1V- or $OMV_{Yp}$-Bla-V–vaccinated mice were higher than those in PBS-vaccinated mice, but significantly less than those in $OMV_{YptbS44}$-Bla-V–immunized mice (Fig. 5*D*). There were no measurable increases in the actual numbers of IFN-γ– and IL-17A–producing $CD8^+$ T cells among the immunized mice after pulmonary challenge (*SI Appendix*, Fig. S7). When compared to the other immunized mice, only the number of TNF-α–producing $CD8^+$ T cells in $OMV_{YptbS44}$-Bla-V–vaccinated mice increased substantially (*SI Appendix*, Fig. S7). Our results demonstrated that $OMV_{YptbS44}$-Bla-V vaccination elicited more robust *Y. pestis*-specific $CD4^+$ T cell responses in mice than F1V or $OMV_{Yp}$-Bla-V vaccination.

**$OMV_{YptbS44}$-Bla-V Vaccination Restricts the Bacterial Burden and Lung Inflammation after Pulmonary *Y. pestis* Infection.** Based on the aforementioned protection and immune responses observed in vaccinated mice, we determined the correlation between animal survival and host responses by monitoring the lung bacterial burden, histopathology, and cytokine production in bronchoalveolar lavage fluid (BALF) after pulmonary *Y. pestis* challenge. On day 2 postinfection, the lungs of PBS-immunized mice had strikingly high *Y. pestis* titers (mean 8.1 $\log_{10}$ CFU/g tissue). *Y. pestis* disseminated into the liver (mean 4.7 $\log_{10}$ CFU/g tissue) and spleen (mean 3.8 $\log_{10}$ CFU/g tissue) at significant bacterial titers (Fig. 6*A*). In F1V-vaccinated mice, lungs had moderate bacterial titers (mean 3.8 $\log_{10}$ CFU/g tissue), but the liver and spleen had limited bacterial titers (Fig. 6*A*). High lung bacterial numbers were also detected in the $OMV_{Yp}$-Bla-V–vaccinated mice, moderate bacterial numbers were found in the liver, while limited bacteria were detected in the spleen. No *Y. pestis* was detected in the lungs of $OMV_{YptbS44}$-Bla-V–vaccinated mice, and no bacteria disseminated to the liver or spleen (Fig. 6*A*).

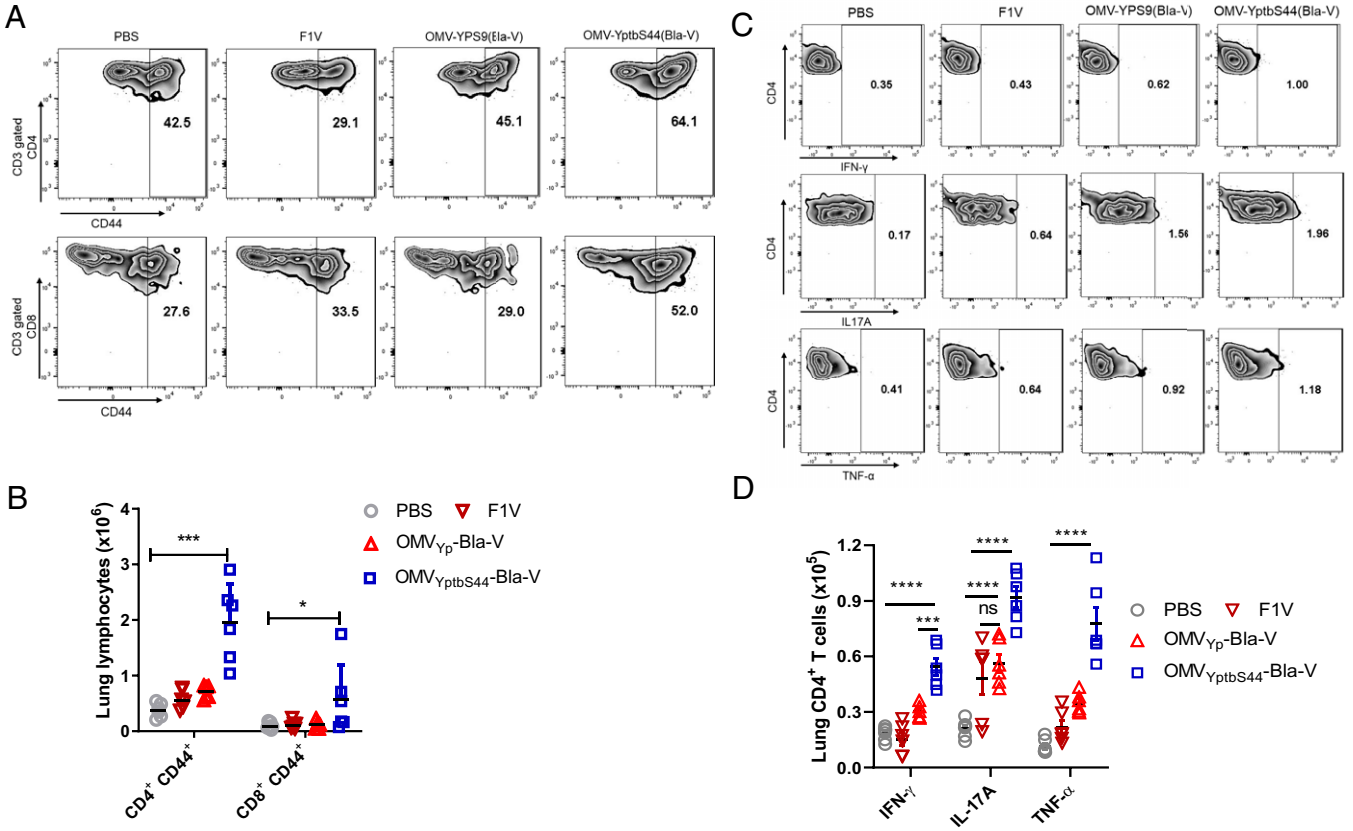


**Fig. 5.** Analysis of lung T cell responses after pulmonary *Y. pestis* infection. Swiss Webster mice ($n$ = 6) were immunized intramuscularly with 40 μg of $OMV_{YptbS44}$-Bla-V/100 μL of PBS, 40 μg of $OMV_{Yp}$-Bla-V/100 μL of PBS, 10 μg of F1V/Alhydrogel/100 μL of PBS, or Alhydrogel alone/100 μL of PBS (negative control) and then boosted on day 21 after the priming immunization. On day 42 after the initial immunization, mice were intranasally challenged with $5 \times 10^6$ CFU of *Y. pestis* KIM6(pCD1Ap) ($Pgm^-$). Three days postinfection, the lungs were aseptically isolated for analysis of the T cell response (*Materials and Methods*). (*A*) Representative flow cytometry profiles for $CD4^+$ $CD44^+$ T cells in different mice. (*B*) Quantification of $CD4^+$ $CD44^+$ T cell numbers in the lungs of mice. (*C*) Representative flow cytometry profiles for $CD4^+$ T cells producing IFN-γ, IL-17, or TNF-α in the lungs of different immunized mice. (*D*) Quantification of $CD4^+$ IFN-$\gamma^+$, $CD4^+$ IL-$17^+$, and $CD4^+$ TNF-$\alpha^+$ cell numbers in the lungs of mice. Each symbol represents a data point obtained from an individual mouse, with the mean ± SD indicated. The experiments were performed twice, and data were combined for analysis. The statistical significance of differences among the groups was analyzed by two-way multivariate ANOVA with Tukey's post hoc test: ns, no significance; *$P < 0.05$; **$P < 0.01$; ***$P < 0.001$; ****$P < 0.0001$. Interferon, (INF)-γ; tumor necrosis factor, (TNF)-α.

Moreover, lung histopathological changes were examined at 48 h postpulmonary *Y. pestis* infection. Large lobar pulmonary lesions in the lungs with neutrophil infiltration and tissue consolidation were observed in PBS- and $OMV_{Yp}$-Bla-V–immunized mice. These animals developed interstitial pneumonia with marked increases in alveolar hemorrhage, perivascular edema, and inflammation (Fig. 6*B*). The lungs of F1V-immunized mice showed smaller nodular inflammatory lesions within the alveoli, whereas the lungs of $OMV_{YptbS44}$-Bla-V–immunized mice looked unremarkable compared with uninfected lung tissue (Fig. 6*B* and *SI Appendix*, Fig. S8). Lung histopathological scores from different immunized mice were estimated using rough grade scales (0, absent; 1, slight; 2, moderate; and 3, severe). Results showed both scores from PBS- and $OMV_{YptbS44}$-Bla-V–immunized mice were similar but substantially higher than those from F1V- or $OMV_{Yp}$-Bla-V–immunized mice after 48 h infection (Fig. 6*C*). The score from $OMV_{Yp}$-Bla-V–immunized mice was the lowest among all groups (Fig. 6*C*). Additionally, dramatically increased levels of proinflammatory cytokines (IL-1β and IL-6) and chemokines (G-CSF and KC) were secreted into the BALF of PBS- and $OMV_{Yp}$-Bla-V–immunized mice on day 2 postinfection in comparison to the levels in the BALF of uninfected sham mice. The levels of these cytokines and chemokines in the BALF of F1V-immunized mice at day 2 postinfection were slightly higher than those in the preinfected mice. However, there were no significant differences in the levels of these cytokines and chemokines in the BALF of $OMV_{YptbS44}$-Bla-V–immunized mice between preinfection and postinfection (Fig. 6*D*). Thus, high lung bacterial burdens led to high production of proinflammatory cytokines and chemokines correlated with dramatic lung damage, leading to rapid death (Fig. 2*C*).

## Discussion

Due to the absence of *lpxL* and *pagP*, *Y. pestis* mainly synthesizes low toxic tetraacylated lipid A with weak stimulatory activity via TLR4 interaction at 37 °C and can evade innate immune surveillance (32, 33), whereas the presence of *lpxP* in *Y. pestis* allows the addition of palmitoleate (C16:1) to form hexaacylated lipid A at room temperature or below (17, 18). Unlike *Y. pestis*, Yptb has a full set of lipid A biosynthesis enzymes and mainly produces hexaacylated lipid A, a critical moiety of endotoxin at both room and mammalian temperatures (18, 25, 34). In comparison to Δ*tolR* Yptb, the YptbS44 mutant strain with the *lpxE* insertion demonstrated the generation of monophosphate lipid A species and a significant reduction in the TLR4 stimulation of OMVs (Fig. 1*E*). However, the remaining unmodified hexaacylated lipid A in OMVs from YptbS44, due to incomplete removal of the 1-phosphate group

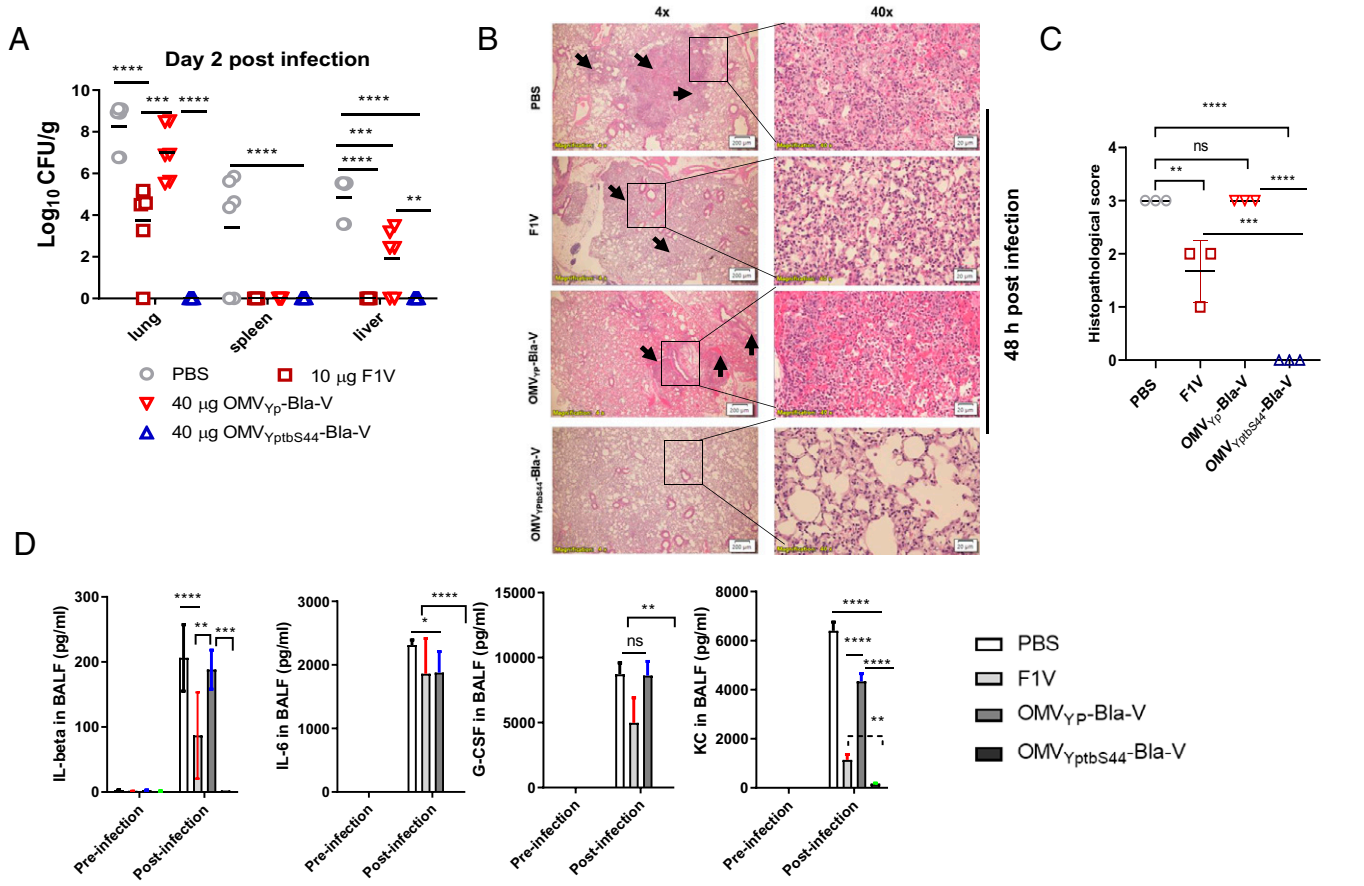


**Fig. 6.** Lung responses after *Y. pestis* pulmonary infection. Swiss Webster mice ($n$ = 6) were immunized intramuscularly with 40 μg of $OMV_{YptbS44}$-Bla-V/100 μL of PBS, 40 μg of $OMV_{Yp}$-Bla-V/100 μL of PBS, 10 μg of F1V/Alhydrogel/100 μL of PBS, or Alhydrogel alone/100 μL of PBS (negative control) and then boosted on day 21 after the priming immunization. On day 42 after the initial immunization, mice were intranasally challenged with 50 $LD_{50}$ of *Y. pestis* $KIM6^+$ (pCD1Ap). At 48 h postchallenge, different tissues (lungs, liver, and spleen) and the BALF were collected from euthanized mice. (*A*) The bacterial burden was evaluated in the lungs, liver, and spleen. The experiments were performed twice, and the data were combined for analysis. (*B*) Lung histopathological analysis of representative mice from each group 48 h after pulmonary *Y. pestis* infection. The lungs were microscopically examined and imaged at 4× magnification (Scale bar, 200 nm.) and 40× magnification (Scale bar, 20 nm.). (*C*) The pathological scores of lung tissue sections after infection. Inflammatory cell infiltration (shown with black arrows) and increased alveolar wall thickness were observed in the lungs of mice infected via the i.n. route at 48 h postinfection. Each tissue section was observed and scored by a semiquantitative method (0, absent; 1, slight; 2, moderate; and 3, severe) under a light microscope with a minimum four-point assessment of pathological conditions. (*D*) Comparison of cytokine and chemokine levels in the BALF from mice with or without pulmonary *Y. pestis* challenge. PBS-, F1V-, 40 μg $OMV_{Yp}$-Bla-V–, or 40 μg $OMV_{YptbS44}$-Bla-V–immunized Swiss Webster mice ($n$ = 6) were infected i.n. with 50 $LD_{50}$ of *Y. pestis* $KIM6^+$(pCD1Ap). Groups of immunized mice injected with PBS served as negative controls. The BALF from each euthanized mouse was collected at 48 h postinfection, filtered through a 0.22-μm syringe filter, and checked for sterility before transfer to a BSL2 laboratory for analysis. ELISA kits (Invitrogen) were used to detect cytokines and chemokines, such as IL-1β, IL-6, G-CSF, and KC, in the BALF collected from mice according to the manufacturer's instructions. The experiments were performed twice, and the data were combined for analysis. The statistical significance of differences among the groups was analyzed by two-way multivariate ANOVA with a Tukey's post hoc test. ****$P$ < 0.0001. Interleukin (IL); granulocyte CSF (G-CSF); KC/CXCL1.

(*SI Appendix*, Fig. S2 *B* and *C*), led to significant reactogenicity that manifested retardation of animal weight gain (Figs. 2*B* and 3*B*) and increased levels of IL-6 and IL-1β (*SI Appendix*, Fig. S3*C*) after immunization. High induction of proinflammatory cytokines (IL-6 and IL-1β) is correlated with toxicity and reactogenicity (35, 36). MS data showed that the major lipid A species in $OMV_{YptbS44}$-Bla-V were penta- and hexaacylated lipid A with two 4-amino-4-deoxy-L-arabinose (L-Ara4N) moieties (*SI Appendix*, Fig. S2 *A–C*). So, occupancy of L-Ara4N in the 1-phosphate position may prevent LpxE access for catalysis. In Yptb, the presence of an intact *pmrHFIJKLM* (also termed *arnBCADTEF*) operon (37) contributes to the L-Ara4N addition to phosphate groups in lipid A of Yptb and its OMVs. Therefore, we will determine whether eliminating the addition of L-Ara4N by adding the *arnT* deletion can enhance 1-dephosphorylation of lipid A in future studies. In addition, introducing both *lpxP* and *lpxL* mutations on top of the YptbS44 generated a new mutant, YptbS45, which predominantly synthesizes a low toxic monophosphate tetraacylated lipid A without 4-amino-4-deoxy-L-arabinose (L-Ara4N) moieties (*SI Appendix*, Fig. S2*E*). The result suggests that removing fatty acid chains of lipid A may affect the modification of L-Ara4N. So, comprehensive studies in the Yptb lipid A modification will be conducted further.

In gram-negative bacteria, such as *Haemophilus influenzae*, *Vibrio cholerae*, *E. coli*, and others, disruption of *vacJ*, *yrbE*, or *nlpI* results in excessive OMV production (23, 24). However, similar observations were not found for the Yptb $PB1^+$ strain with individual mutation of *vacJ*, *yrbE*, or *nlpI* (Fig. 1*A*), even though the protein encoded by each respective gene had high homology among the strains. Therefore, the roles of these genes in Yptb $PB1^+$ might be different from those in other bacterial species. Additionally, OMVs were isolated from Yptb grown at its favorable temperature (28 °C), not at 37 °C used by the aforementioned bacteria, which suggests that cultivation temperatures may affect bacterial membrane curvature in these *vacJ*, *yrbE*, or *nlpI* mutant strains. However, deletion of *tolR* in

Yptb resulted in a variety of phenotypic changes and high production of OMVs (Fig. 1 *A* and *B*), which was consistent with previous studies (22, 23). In addition, previous studies have shown that bacterial OMVs contain periplasmatic and cytosolic proteins and nucleic acids, but the presence of cytoplasmic contents within OMVs remains elusive (38). Similarly, our proteomic analysis of $OMV_{YptbS44}$-Bla-V enclosed a high amount of LcrV antigen delivered by T2SS, as well as a large portion of cytosolic proteins (*SI Appendix*, Fig. S1*C* and Dataset S1). We speculate that lipid A modifications and the *tolR* mutation may promote the package of cytoplasmic contents into OMVs. So far, whether these cytoplasmic contents significantly affect OMV immunogenicity is uncertain.

In general, mucosal administration of vaccines can efficiently induce mucosal immune responses, whereas parenteral administration of vaccines generally induces poor mucosal immunity, leading to relatively low protection against infection at mucosal surfaces (39). Jones et al. reported that i.n. immunization with Protollin-F1-V provided great protection against lethal aerosolized plague infection in mice (40). However, unlike i.m. $OMV_{YptbS44}$-Bla-V immunization, which offered great protection against both pneumonic plague and bubonic plague (Fig. 2 *C*–*E* and *SI Appendix*, Fig. S3 *E* and *F*), the protection against both pneumonic plague and bubonic plague induced by i.n. $OMV_{YptbS44}$-Bla-V immunization occurred in a dose-dependent manner (Fig. 3 *C* and *D* and *SI Appendix*, Fig. S4 *C* and *D*). Since vaccines deposited directly on mucosal surfaces confront the same host defenses as microbial pathogens, vaccines might be diluted in mucosal secretions, captured in mucus gels, attacked by proteases and nucleases, or excluded by epithelial barriers (39). Thus, relatively large doses of vaccine, such as 16 μg of $OMV_{YptbS44}$-Bla-V instead of 8 or 4 μg of OMVs, are required to overcome these barriers and provide effective protection against pneumonic plague. In addition, i.n. immunization with 16 μg of $OMV_{YptbS44}$-Bla-V only provided partial protection against bubonic plague (*SI Appendix*, Fig. S4*C*), even though this immunization induced levels of anti-LcrV and anti-F1 antibody titers (*SI Appendix*, Fig. S5) similar to those induced by i.m. immunization with 40 μg of $OMV_{YptbS44}$-Bla-V (Fig. 4). Due to animal death caused by i.n. immunization with 16 μg of $OMV_{YptbS44}$-Bla-V, the safety and efficacy of i.n. OMV vaccination remain to be established. However, the detailed reasons will be investigated in our future studies to reveal why i.n. immunization with the current form of OMVs failed to induce robust protection against bubonic plague. In addition to high induction of anti-LcrV IgG titers, higher anti-LcrV IgM titers were induced by i.m. immunization with 40 μg of $OMV_{YptbS44}$-Bla-V than by immunization with 40 μg of $OMV_{Yp}$-Bla-V or F1V (Fig. 4 *A* and *C*), which might correlate with protection against plague challenge (Figs. 2 and 3). IgM has been demonstrated to play protective roles in extracellular and intracellular bacterial infections (41, 42) and to facilitate the removal of foreign pathogens through efficient agglutination (43). High levels of anti-F1 IgM are induced by the capsular F1 antigen of *Y. pestis* recognized by B1b cells and perform a significant role in protecting against plague challenge (44). Thus, the high levels of anti-LcrV IgM induced by immunization with 40 μg of $OMV_{YptbS44}$-Bla-V might contribute to complete antiplague protection. The defined role of IgM in protection against *Y. pestis* infection will be investigated in future studies.

Similar to our previous study (10), OMV vaccination induced a more balanced Th1/Th2 immune response than subunit F1V vaccination (Fig. 3 *B* and *F*), implicating the induction of cellular immune responses. Antibody and cellular immune responses are required to synergistically defend against pulmonary *Y. pestis* infection (45–47). IL-17 also contributes to cell-mediated defense against pulmonary *Y. pestis* infection (31). Consistent with these previous studies, lung $CD4^+$ T cells from $OMV_{YptbS44}$-Bla-V–immunized mice produced higher levels of Th1 and Th17 cytokines (IFN-γ, IL-17, or TNF-α) than those from F1V- or $OMV_{Yp}$-Bla-V–immunized mice after *Y. pestis* infection (Fig. 5*D*). Thus, potent Th1 and Th17 cell responses induced by $OMV_{YptbS44}$-Bla-V vaccination might be one of the possible mechanisms providing superior protection against both pneumonic plague and bubonic plague. In naive mice, the proinflammatory phase (48 h postinfection) is characterized by dramatic increases in the titers of bacteria and levels of cytokines (IL-1β and IL-6) and chemokines (G-CSF and KC) accompanied by massive neutrophil influx into the lungs and alveolar spaces, resulting in acute lethal pneumonia (48, 49). Our data showed that the responses in PBS-immunized mice on day 2 postinfection (Fig. 6) were consistent with previous observations (50). In addition, our data suggested that the high levels of humoral and T cell responses in mice mounted in response to immunization (Figs. 4 and 5) were strongly correlated with rapid bacterial clearance, unremarkable tissue damage in the lungs, and low secretion of inflammatory cytokines in the BALF (Fig. 6). As previous studies have reported (50, 51), the massive infiltration of neutrophils into the alveolar lumina in response to an increased bacterial burden led to necrotic lethal pneumonia in PBS- and $OMV_{Yp}$-Bla-V–immunized mice (Fig. 6 *A* and *B*). However, the infiltration of neutrophils (Fig. 6*B*) and production of proinflammatory cytokines/chemokines (Fig. 6*C*) were extremely low in $OMV_{YptbS44}$-Bla-V–immunized mice, so complete clearance of bacteria on day 2 postinfection could rapidly return the lungs to homeostasis. The underlying mechanisms of how humoral and T cell immune responses coordinate with the recruitment of innate cells for pneumonic protection will be studied further once we have an optimal *Yersinia* OMV vaccine candidate.

In our previous study, χ10061 with chromosomal insertion of the *Y. pestis caf1R-caf1M-caf1A-caf1* operon was found to produce large amounts of F1 antigen upon 37 °C induction (15). The YptbS44 strain containing additional mutations compared with the χ10061 strain showed significantly diminished F1 synthesis at 37 °C for unknown reasons. However, the YptbS44 strain harboring an *lcrV* expression plasmid exhibited high synthesis of LcrV and high amount of LcrV enclosed in OMVs (Fig. 1*C*), so a recombinant Yptb strain tailored a *caf1* expression plasmid would increase the amount of F1 antigen enclosed in OMVs which manifest enhanced immunogenicity. Additionally, we will attempt to include more *Y. pestis* protective antigens, such as Psn (52) or YscF (53) in the optimized OMVs to maximize immunogenicity in future studies.

Altogether, our studies showed that a remodeled Yptb strain harboring an *lcrV* expression plasmid could dramatically increase the production of OMVs enclosing large amounts of LcrV compared to a previous recombinant *Y. pestis* strain. The $OMV_{YptbS44}$-Bla-V immunization by i.m. injection induced robust humoral and cellular immune responses and afforded complete protection against high doses of *Y. pestis* infection through either a pulmonary or subcutaneous route; however, significant side effects due to the dominant presence of hexaacylated biphosphate lipid A species were present. However, $OMV_{YptbS45}$-Bla-V isolated from YptbS45(pSMV13) with additional *lpxP* and *lpxL* mutations predominantly containing monophosphate tetraacylated lipid A exhibited dramatically low toxicity (*SI Appendix*, Figs. S2*F* and S3*C*) and still retained high immunogenicity (Fig. 2*C* and

*SI Appendix*, Fig. S3 *D* and *E*). Therefore, further optimized Yptb OMVs could be a promising and effective next-generation plague vaccine candidate.

## Materials and Methods

**Strains, Plasmids, Culture Conditions, and Molecular Procedures.** All bacterial strains and plasmids used in this study are listed in *SI Appendix*, Table S1. All bacterial cultures and molecular procedures applied in this study are described in *SI Appendix*.

**OMV Isolation and Analysis.** OMVs were isolated from *Y. pestis* and Yptb strains as described previously (10). A brief procedure and analysis are included in *SI Appendix*.

**Lipid A Isolation and Analysis.** The detailed procedures for lipid A isolation from Yptb and its OMVs and lipid A analysis using normal-phase liquid chromatography/electrospray ionization-mass spectrometry (NPLC/ESI-MS) were conducted as described previously (54, 55) with minor modifications (*SI Appendix*).

**Animal Experiments.** All animal studies were performed in accordance with the NIH "Guide for the Care and Use of Laboratory Animals" and approved by the Institutional Animal Care and Use Committee at Albany Medical College (IACUC protocol# 20-01001). Six-week-old male and female Swiss Webster mice were purchased from Charles River Laboratories and acclimated for 1 wk after arrival. Groups of mice were either i.m. or i.n. immunized with OMVs. Vaccination with F1V/Alhydrogel or PBS/Alhydrogel was used as an experimental control. Booster vaccination was then performed 3 wk after the initial vaccination. Blood was collected via the submandibular veins every 2 wk to harvest serum for antibody analysis. At 42 d after the initial vaccination, animals were anesthetized with 100 μL of ketamine/xylazine mixture (25 mg/mL ketamine plus 1 mg/mL xylazine) and challenged i.n. with virulent *Y. pestis* in 40 μL of PBS to mimic pneumonic plague. Animals were challenged s.c. with *Y. pestis* KIM6$^+$(pCD1Ap) in 100 μL of PBS by front neck injection to mimic bubonic plague. All infected animals were monitored over a 15-d period.

For determination of the bacterial burden after pulmonary *Y. pestis* infection, animals were euthanized with an overdose of sodium pentobarbital. The lungs, liver, and spleen were removed at the indicated time and homogenized in ice-cold PBS (pH 7.4) using a bullet blender (Bullet Blender Blue) at power 7 for 2 min. Serial dilutions of each organ homogenate were plated on HIB agar, and each count was confirmed with duplicate plates with three dilutions to determine the bacterial titer per gram of tissue.

**Antibody and Cytokine Analysis.** An enzyme-linked immunosorbent assay (ELISA) was used to assay the titers of antibodies against LcrV and F1 in the serum (*SI Appendix*). A mouse cytokine/chemokine ELISA kit (Invitrogen) was used to detect cytokines/chemokines in the BALF and serum was collected from mice according to the manufacturer's instructions.

**Measurement of T Cell Responses.** The activation and cytokine production of T cells in the lungs were evaluated as described previously (30) with minor modifications. Immunized mice underwent pulmonary challenge with $5 \times 10^6$ CFU of *Y. pestis* KIM6(pCD1Ap) (Pgm$^-$) and were euthanized on day 3 postinfection. The lung cells were collected and stained with different fluorochrome-labeled antibodies for analysis (*SI Appendix*). Events were acquired on BD flow cytometers (LSRII) with FACSDiva software and analyzed using FlowJo v.10.

**Histopathology.** Groups of three mice were infected intranasally with $5 \times 10^3$ CFU of *Y. pestis* KIM6$^+$(pCD1Ap). At 48 h postinfection, the mice were euthanized with pentobarbital sodium (100 mg/kg). The lungs were collected and fixed in 10% formalin overnight before being embedded in paraffin. Lungs from uninfected mice were used as experimental controls. Three-micrometer sections of tissue were stained either with hematoxylin/eosin or by immunostaining before being examined as described previously (50).

**Statistical Analysis.** Each experiment included a significant number (minimum of three) of biological replicates, with two to three replicates performed in a synchronized fashion to establish reproducibility. Statistical analyses of comparisons of data among groups were performed with one-way ANOVA/univariate or two-way ANOVA with Tukey's post hoc tests. The log-rank (Mantel–Cox) test was used for survival analysis. All data were analyzed using GraphPad PRISM 8.0 software. The data are represented as the mean ± SD (ns, no significance; $*P < 0.05$; $**P < 0.01$; $***P < 0.001$; $****P < 0.0001$).

**Data Availability.** All study data are included in the article and/or supporting information.

**ACKNOWLEDGMENTS.** We thank Mr. Ravindra Thakkar (Nanotechnology Innovation Center of Kansas State University) for taking the OMV images via electron microscopy, Dr. Haian Zheng (Albany College of Pharmacy and Health Sciences) for helping dynamic light scattering of OMVs, and Dr. Saugata Majumder for assisting animal challenge. *Y. pestis* F1-V Fusion Protein, Monomer-Enriched Antigen, Recombinant from *E. coli*, and NR-2561 were obtained through BEI Resources, NIAID, and NIH. This work was supported by NIH Grants R21AI139703 and R01AI125623 to W.S. and R01AI148366 to Z.G.

Author affiliations: [a]Department of Immunology and Microbial Disease, Albany Medical College, Albany, NY 12208; [b]Department of Pharmaceutical Sciences, Eugene Applebaum College of Pharmacy/Health Sciences, Wayne State University, Detroit, MI 48201; [c]Department of Biochemistry, Duke University Medical Center, Durham, NC 27710; and [d]Department of Infectious Diseases and Immunology, College of Veterinary Medicine, University of Florida, Gainesville, FL 32611

1. R. D. Perry, J. D. Fetherston, *Yersinia pestis*–etiologic agent of plague. *Clin. Microbiol. Rev.* **10**, 35–66 (1997).
2. K. L. Gage, M. Y. Kosoy, Natural history of plague: Perspectives from more than a century of research. *Annu. Rev. Entomol.* **50**, 505–528 (2005).
3. D. E. Biggins, D. A. Eads, Prairie dogs, persistent plague, flocking fleas, and pernicious positive feedback. *Front. Vet. Sci.* **6**, 75 (2019).
4. The Centers for Disease Control and Prevention, 4 deaths, 15 cases of bubonic plague in U.S. this year. https://cbs4indy.com/2015/10/22/cdc-4-deaths-15-cases-of-bubonic-plague-in-u-s-this-year/. Accessed 22 October 2015.
5. The World Health Organization, Plague – Madagascar. https://www.who.int/csr/don/15-november-2017-plague-madagascar/en/. Accessed 15 November 2017.
6. R. Dai *et al.*, Human plague associated with Tibetan sheep originates in marmots. *PLoS Negl. Trop. Dis.* **12**, e0006635 (2018).
7. T. J. Welch *et al.*, Multiple antimicrobial resistance in plague: An emerging public health risk. *PLoS One* **2**, e309 (2007).
8. L. Radnedge, P. G. Agron, P. L. Worsham, G. L. Andersen, Genome plasticity in *Yersinia pestis*. *Microbiology (Reading)* **148**, 1687–1698 (2002).
9. W. Sun, A. K. Singh, Plague vaccine: Recent progress and prospects. *NPJ Vaccines* **4**, 11 (2019).
10. X. Wang, A. K. Singh, X. Zhang, W. Sun, Induction of protective anti-plague immune responses by self-adjuvanting bionanoparticles derived from engineered *Yersinia pestis*. *Infect. Immun.* **88**, e00081–e00020 (2020).
11. P. S. Chain *et al.*, Insights into the evolution of *Yersinia pestis* through whole-genome comparison with *Yersinia pseudotuberculosis*. *Proc. Natl. Acad. Sci. U.S.A.* **101**, 13826–13831 (2004).
12. A. R. Gorringe, R. Pajón, Bexsero: A multicomponent vaccine for prevention of meningococcal disease. *Hum. Vaccin. Immunother.* **8**, 174–183 (2012).
13. J. Hinnebusch *et al.*, Murine toxin of *Yersinia pestis* shows phospholipase D activity but is not required for virulence in mice. *Int. J. Med. Microbiol.* **290**, 483–487 (2000).
14. A. J. Caulfield, M. E. Walker, L. M. Gielda, W. W. Lathem, The Pla protease of *Yersinia pestis* degrades fas ligand to manipulate host cell death and inflammation. *Cell Host Microbe* **15**, 424–434 (2014).
15. W. Sun, S. Sanapala, H. Rahav, R. Curtiss, 3rd, Oral administration of a recombinant attenuated *Yersinia pseudotuberculosis* strain elicits protective immunity against plague. *Vaccine* **33**, 6727–6735 (2015).
16. C. Watters, D. Fleming, D. Bishop, K. P. Rumbaugh, Host responses to biofilm. *Prog. Mol. Biol. Transl. Sci.* **142**, 193–239 (2016).
17. C. R. Raetz, C. Whitfield, Lipopolysaccharide endotoxins. *Annu. Rev. Biochem.* **71**, 635–700 (2002).
18. R. Rebeil *et al.*, Characterization of late acyltransferase genes of *Yersinia pestis* and their role in temperature-dependent lipid A variation. *J. Bacteriol.* **188**, 1381–1388 (2006).
19. W. Sun *et al.*, Pathogenicity of *Yersinia pestis* synthesis of 1-dephosphorylated lipid A. *Infect. Immun.* **81**, 1172–1185 (2013).
20. N. Garçon, M. Van Mechelen, Recent clinical experience with vaccines using MPL- and QS-21-containing adjuvant systems. *Expert Rev. Vaccines* **10**, 471–486 (2011).
21. I. Sonntag, H. Schwarz, Y. Hirota, U. Henning, Cell envelope and shape of *Escherichia coli*: Multiple mutants missing the outer membrane lipoprotein and other major outer membrane proteins. *J. Bacteriol.* **136**, 280–285 (1978).
22. A. Bernadac, M. Gavioli, J. C. Lazzaroni, S. Raina, R. Lloubès, *Escherichia coli* tol-pal mutants form outer membrane vesicles. *J. Bacteriol.* **180**, 4872–4878 (1998).
23. S. Roier *et al.*, A novel mechanism for the biogenesis of outer membrane vesicles in Gram-negative bacteria. *Nat. Commun.* **7**, 10515 (2016).
24. C. Schwechheimer, D. L. Rodriguez, M. J. Kuehn, NlpI-mediated modulation of outer membrane vesicle production through peptidoglycan dynamics in *Escherichia coli*. *MicrobiologyOpen* **4**, 375–389 (2015).
25. R. Rebeil, R. K. Ernst, B. B. Gowen, S. I. Miller, B. J. Hinnebusch, Variation in lipid A structure in the pathogenic yersiniae. *Mol. Microbiol.* **52**, 1363–1373 (2004).

26. M. Hellfritzsch, R. Scherließ, Mucosal vaccination via the respiratory tract. *Pharmaceutics* **11**, 375 (2019).
27. T. Germann *et al.*, Interleukin-12 profoundly up-regulates the synthesis of antigen-specific complement-fixing IgG2a, IgG2b and IgG3 antibody subclasses in vivo. *Eur. J. Immunol.* **25**, 823–829 (1995).
28. S. T. Smiley, Cell-mediated defense against *Yersinia pestis* infection. *Adv. Exp. Med. Biol.* **603**, 376–386 (2007).
29. R. C. Budd *et al.*, Distinction of virgin and memory T lymphocytes. Stable acquisition of the Pgp-1 glycoprotein concomitant with antigenic stimulation. *J. Immunol.* **138**, 3120–3129 (1987).
30. F. M. Szaba *et al.*, D27-pLpxL, an avirulent strain of *Yersinia pestis*, primes T cells that protect against pneumonic plague. *Infect. Immun.* **77**, 4295–4304 (2009).
31. J. S. Lin, L. W. Kummer, F. M. Szaba, S. T. Smiley, IL-17 contributes to cell-mediated defense against pulmonary *Yersinia pestis* infection. *J. Immunol.* **186**, 1675–1684 (2011).
32. C. E. Chandler *et al.*, Early evolutionary loss of the lipid A modifying enzyme PagP resulting in innate immune evasion in *Yersinia pestis*. *Proc. Natl. Acad. Sci. U.S.A.* **117**, 22984–22991 (2020).
33. S. W. Montminy *et al.*, Virulence factors of *Yersinia pestis* are overcome by a strong lipopolysaccharide response. *Nat. Immunol.* **7**, 1066–1073 (2006).
34. W. Sun *et al.*, LcrV delivered via type III secretion system of live attenuated *Yersinia pseudotuberculosis* enhances immunogenicity against pneumonic plague. *Infect. Immun.* **82**, 4390–4404 (2014).
35. J. Geurtsen *et al.*, Lipopolysaccharide analogs improve efficacy of acellular pertussis vaccine and reduce type I hypersensitivity in mice. *Clin. Vaccine Immunol.* **14**, 821–829 (2007).
36. N. Muñoz-Wolf, E. C. Lavelle, A Guide to IL-1 family cytokines in adjuvanticity. *FEBS J.* **285**, 2377–2401 (2018).
37. L. E. Johnson, "*The pmrHFIJKLM Operon in Yersinia pseudotuberculosis Enhances Resistance to CCL28 and Promotes Phagocytic Engulfment by Neutrophils*," PhD thesis, Brigham Young University, Provo, UT (2016).
38. M. Toyofuku, N. Nomura, L. Eberl, Types and origins of bacterial membrane vesicles. *Nat. Rev. Microbiol.* **17**, 13–24 (2019).
39. M. R. Neutra, P. A. Kozlowski, Mucosal vaccines: The promise and the challenge. *Nat. Rev. Immunol.* **6**, 148–158 (2006).
40. T. Jones *et al.*, Intranasal Protollin/F1-V vaccine elicits respiratory and serum antibody responses and protects mice against lethal aerosolized plague infection. *Vaccine* **24**, 1625–1632 (2006).
41. K. M. Haas, J. C. Poe, D. A. Steeber, T. F. Tedder, B-1a and B-1b cells exhibit distinct developmental requirements and have unique functional roles in innate and adaptive immunity to *S. pneumoniae*. *Immunity* **23**, 7–18 (2005).
42. A. F. Cunningham *et al.*, *Salmonella* induces a switched antibody response without germinal centers that impedes the extracellular spread of infection. *J. Immunol.* **178**, 6200–6207 (2007).
43. N. R. Cooper, G. R. Nemerow, J. T. Mayes, Methods to detect and quantitate complement activation. *Springer Semin. Immunopathol.* **6**, 195–212 (1983).
44. Y. Levy *et al.*, Targeting of the *Yersinia pestis* F1 capsular antigen by innate-like B1b cells mediates a rapid protective response against bubonic plague. *NPJ Vaccines* **3**, 52 (2018).
45. S. T. Smiley, Immune defense against pneumonic plague. *Immunol. Rev.* **225**, 256–271 (2008).
46. B. Li *et al.*, Humoral and cellular immune responses to *Yersinia pestis* infection in long-term recovered plague patients. *Clin. Vaccine Immunol.* **19**, 228–234 (2012).
47. M. A. Parent *et al.*, Cell-mediated protection against pulmonary *Yersinia pestis* infection. *Infect. Immun.* **73**, 7304–7310 (2005).
48. W. W. Lathem, S. D. Crosby, V. L. Miller, W. E. Goldman, Progression of primary pneumonic plague: A mouse model of infection, pathology, and bacterial transcriptional activity. *Proc. Natl. Acad. Sci. U.S.A.* **102**, 17786–17791 (2005).
49. S. L. Agar *et al.*, Characterization of a mouse model of plague after aerosolization of *Yersinia pestis* CO92. *Microbiology (Reading)* **154**, 1939–1948 (2008).
50. R. D. Pechous, V. Sivaraman, P. A. Price, N. M. Stasulli, W. E. Goldman, Early host cell targets of *Yersinia pestis* during primary pneumonic plague. *PLoS Pathog.* **9**, e1003679 (2013).
51. Y. Vagima *et al.*, Circumventing *Y. pestis* virulence by early recruitment of neutrophils to the lungs during pneumonic plague. *PLoS Pathog.* **11**, e1004893 (2015).
52. C. G. Branger *et al.*, Evaluation of Psn, HmuR and a modified LcrV protein delivered to mice by live attenuated *Salmonella* as a vaccine against bubonic and pneumonic *Yersinia pestis* challenge. *Vaccine* **29**, 274–282 (2010).
53. J. S. Matson, K. A. Durick, D. S. Bradley, M. L. Nilles, Immunization of mice with YscF provides protection from *Yersinia pestis* infections. *BMC Microbiol.* **5**, 38 (2005).
54. L. R. Joyce, Z. Guan, K. L. Palmer, Phosphatidylcholine biosynthesis in Mitis group streptococci via host metabolite scavenging. *J. Bacteriol.* **201**, e00495-19 ●(2019).
55. B. K. Tan *et al.*, Discovery of a cardiolipin synthase utilizing phosphatidylethanolamine and phosphatidylglycerol as substrates. *Proc. Natl. Acad. Sci. U.S.A.* **109**, 16504–16509 (2012).
56. W. Sun *et al.*, A live attenuated strain of *Yersinia pestis* KIM as a vaccine against plague. *Vaccine* **29**, 2986–2998 (2011).